Energy pile displacements due to cyclic thermal loading at different mechanical load levels

Rafai, Mouadh; Salciarini, Diana; Vardon, Philip J.

DOI
10.1007/s11440-025-02556-4

Publication date
2025

Document Version
Final published version

Published in
Acta Geotechnica

Acta Geotechnica
https://doi.org/10.1007/s11440-025-02556-4

RESEARCH PAPER

Energy pile displacements due to cyclic thermal loading at different mechanical load levels

Mouadh Rafai[1,2] · Diana Salciarini[1] · Philip J. Vardon[2]

Received: 22 July 2024 / Accepted: 22 January 2025

Abstract
The effect of the load level on long-term thermally induced pile displacements and the impact of cyclic thermal loads on the bearing capacity of energy piles are investigated via a full-scale in situ test in Delft, The Netherlands. The pile was loaded to a specific target of 0, 30, 40, or 60% of its calculated ultimate bearing capacity. At the end of each loading step, up to ten cooling–natural heating cycles were applied. The pile behavior during monotonic cooling and cyclic cooling–natural heating in terms of the displacement along the pile is reported, with a focus on permanent displacements. During monotonic (pile/ground) cooling, a settlement of the pile head and an uplift of the pile segment near the pile tip were observed in all four tests. In addition, under higher mechanical load, the pile head displacement was larger while the uplift was lower due to the imposed mechanical load. During cyclic thermal load, under zero mechanical load, pile head displacement was fully reversible while permanent uplift of the lowest pile segment was observed and attributed mainly to the permanent dragdown of the surrounding soil. Under moderate mechanical loads (30 and 40%), thermal cycles induced an irreversible pile head settlement, which stabilized with an increasing number of cycles. In addition, a permanent pile settlement along the pile was observed at the end of these tests. Under high mechanical load (60%), the irreversible settlement along the pile continued to increase with only a slight reduction in rate, being higher compared to moderate mechanical loads. In this test, a normalized pile head settlement of 0.124% was observed after ten thermal cycles. The permanent settlement of the pile under thermo-mechanical loads was mainly attributed to the contraction of sand beneath the pile tip and thermal creep at the soil–structure interface. The pile bearing capacity was observed to increase after thermo-mechanical tests, mainly due to the residual/plastic pile head displacement, which in turn densified sand leading to an increase in tip resistance.

Keywords Bearing capacity · Cyclic thermal loading · Energy pile · Full-scale field tests · Thermo-mechanical response

1 Introduction

Piles are primarily used to support building superstructures. However, due to climate change, economic growth, and energy needs, these piles are becoming increasingly used as a source of heating and cooling buildings by adding tube heat exchangers and incorporating a ground source heat pump to extract heat from the ground during winter and inject it during summer. Such an approach applies additional thermally induced mechanical loads, which can impact both the serviceability and failure of piles. This practice has attracted tremendous attention recently. Numerous studies have been conducted on energy piles, demonstrating their safety and reliability [3, 5, 6, 8, 11, 24, 27, 30, 35, 36, 38, 39, 59]. Pile movements during heating and cooling are inevitable due to the thermal expansion/contraction of the soil and the pile during seasonal, daily, and hourly temperature variations [28, 32, 34, 51], and such displacements—while typically small—can accumulate or have an impact on the bearing capacity of a pile. Pile displacements depend on the applied load, the support provided by the surrounding soils, and the end restraints. In the case of low end-restraint conditions

✉ Mouadh Rafai
mouaadrafai@gmail.com

[1] Department of Civil and Environmental Engineering, University of Perugia, Via G. Duranti, 06125 Perugia, Italy

[2] Faculty of Civil Engineering and Geosciences, Delft University of Technology, 2628CN Delft, The Netherlands

Published online: 22 February 2025

(i.e., floating and semi-floating energy piles), the pile may experience higher axial displacements, hence a large change in mobilized shaft resistance, while having low thermally induced axial stresses. However, in high end-restraint conditions, e.g., end bearing piles, total pile settlements are unlikely to happen, which was confirmed by Stewart and McCartney [57] through an end bearing energy pile test. Moreover, their results revealed a higher thermally induced axial stress near the tip due to the imposed restriction effect.

Laboratory experiments on a semi-floating energy pile in dry sand have shown irreversible pile head settlements due to thermal loads [46, 61]. According to Nguyen et al. [46], the pile head settlement stabilized under lower/moderate mechanical loads (20% and 40% of the estimated bearing capacity of the pile) after 20 thermal cycles, while under high mechanical load, i.e., 60%, it continued to increase even after 20 cycles. Ng et al. [41]; and Ng et al. [45] investigated floating energy piles. Their findings indicated that such piles experienced more irreversible settlement in lightly overconsolidated clay compared to those in soil with a higher overconsolidated ratio (OCR) under cyclic thermal loading. Ng and Ma [40] conducted laboratory tests on energy piles and non-energy piles in sand. Their results demonstrated that the energy pile settlement evolved gradually with time under a constant working load at a reduced rate. Moreover, 30% of this thermally induced settlement was observed in non-energy piles due to the pure applied mechanical load, inducing a mechanical creep over time. Ng et al. [45] reported that the thermally induced irreversible settlement of floating elevated pile groups exceeded both serviceability and ultimate criteria. It should be noted that the aluminum pile was used with a higher thermal expansion coefficient of 22.2×10^{-6} m/(m K), which is about three times that of a concrete pile (8.6×10^{-6} m/(m K)) [6], likely leading to an overestimation in tests compared to field conditions. To investigate the fundamental behavior of soil–structure interfaces, Golchin et al. [20] and Rafai et al. [50] recently studied the effects of thermal cycles on shear creep of the soil–structure interfaces using temperature-controlled shear boxes under constant normal and shear stresses. This can represent the conditions in floating or semi-floating energy piles, as well as in other conditions. Their results showed a continuous thermally induced shear displacement with increasing the number of thermal cycles, indicating a ratcheting pattern. This was found to be dependent on the applied effective (which is the normal stress from the soil surrounding the structure), shear stresses (the pile head load), soil type, and density. Under higher mechanical loads (equivalent to higher pile head load and higher effective stress in soil), higher shear displacement was observed due to thermal cycles. It should be noted that the reported results by Rafai et al. [50] reflect the pure effects of thermal cycles on the shear displacement at the soil–structure interface, as the mechanical creep was fully diminished prior to the application of thermal cycles.

Due to the complexity of the interaction between piles and soil, full-scale in situ experiments have been applied to investigate the thermo-mechanical behavior of energy piles [22, 60].

Considering cyclic thermal loads, Ren et al. [55] investigated an energy pile during monotonic cooling under constant applied mechanical load as well as during cyclic thermal load with no load applied to the pile head. They reported that thermal cycles could reduce the pressure at the soil–structure interface and lead to pile head settlements. A similar observation was reported by Kong et al. [25] through an investigation of semi-floating energy piles. Their results showed that thermal cycles induced decreased horizontal earth pressure, due to the shrinkage effect of surrounding soil, hence reducing shaft resistance, while the tip resistance increased to balance the shaft resistance reduction. Through a full-scale test on a long floating energy pile during up to three cycles of cooling–natural heating and heating–natural cooling under a constant applied mechanical load, Jiang et al. [23] reported that the additional thermally induced permanent settlement is more pronounced in cooling conditions. A similar conclusion was drawn by Jiang et al. [22], investigating a driven energy pile under different mechanical loads and up to four thermal cycles. Moreover, Jiang et al. [22] reported a higher pile settlement under larger mechanical loads. Fang et al. [16] investigated energy piles through full-scale tests under a constant applied mechanical load during four heating–natural recovery thermal cycles. They showed a ratcheting pattern response of pile head displacement due to the imposed thermo-mechanical loads, as also observed in laboratory tests on the soil–structure interface. Wang et al. [60] studied six semi-floating bored energy piles. Each pile was subjected to mechanical loading, heating or cooling, and thermo-mechanical loading, simulating the continuous operation of an energy pile (i.e., monotonic thermal load). Their experimental results show that the largest settlement of the pile head was noted during cooling under a higher mechanical load level. However, Faizal et al. [16] reported a thermo-elastic thermal response at the pile–soil interface under approximately 52% of the estimated ultimate load. This observation was confirmed by Faizal et al. [13]. According to laboratory tests by Yavari et al. [61] and Nguyen et al. [46], the magnitude of thermally induced pile displacements appears to be dependent on the level of the applied mechanical load on the pile head and soil conditions. Since not all the scaling laws are satisfied in such model tests, these results cannot be utilized quantitatively in the design of energy piles. For this reason,

it is paramount to conduct such testing on full-scale energy piles to provide quantitative data. The investigation of the potential effects of multiple thermal cycles on the energy pile–soil interaction mechanism through full-scale tests under long-term cyclic thermal loads is limited. In addition, the impact of thermal cyclic loads on the bearing capacity of the pile through field tests, especially in soft grounds, has received little attention. Furthermore, the existing full-scale tests on energy piles have investigated only pre-cast-driven energy piles [11, 22] and cast in situ energy bored piles [13–15, 26, 55, 58]. Accordingly, the main objective of this paper is to provide a clear understanding of the effect of applied mechanical load on the response of a semi-floating energy pile in soft soil through a series of load paths in a full-scale in situ test. A new type of energy piles called displacement cast in situ energy pile (a Fundex energy pile) was tested as an example of energy piles with the benefit of the surrounding soil being densified during the installation. Four tests were conducted on a fully instrumented stand-alone energy pile under different mechanical loads (0, 30%, 40%, and 60% of the estimated pile bearing capacity) and long-term thermal cycles (up to ten), with an average temperature change magnitude of approximately 10 °C. This is a relatively high temperature change which can simulate multiple years of seasonal GSHP operation [33, 53].

The full-scale in situ test installation and instrumentation are described along with the information on the soil properties. The effects of the applied mechanical load on the pile displacements during monotonic cooling and cyclic cooling–natural heating as well as the effects of cyclic thermal load on the bearing capacity are presented and analyzed.

This paper presents thermally induced pile settlements along the pile during monotonic and cyclic thermal loads, while strain and stress data of this testing program are presented by Rafai et al. [52].

2 Description of field test

A fully instrumented Fundex energy pile was investigated at Delft University of Technology in Delft, the Netherlands. The Fundex energy pile is a displacement cast in situ pile, which is installed in three main phases: (i) A drilling phase, where a steel casing with a sacrificial auger tip, i.e., Fundex cone, attached to its end is rotated into the soil while displacing the soil laterally leading to a densification of the surrounding soil; (ii) In the second phase, the reinforcement cage with a 2U-loop configuration heat exchanger (see Fig. 1a) is placed, and then, the casing is filled with concrete. In the third phase, the sacrificial tip is released; then, the casing is removed. The pile length was 10.3 m (from the pile head to the top of the Fundex cone), and the shank diameter of the pile was 380 mm while the tip diameter was 400 mm, forming an expanded pile (see Fig. 1e).

A deadweight load test frame system was used at the TU Delft test site. This system comprises a steel beam upon which deadweights (a tank filled with water, see Fig. 1c) were placed. One hydraulic jack was utilized to develop a compressive force on the pile head. To monitor the applied force, a load cell was placed between the jack and the frame. The induced pile head settlement was then measured using a linear variable differential transformer (LVDT) (with an accuracy of 0.002 mm) mounted on the pile head as seen in Fig. 1b, with an integrated thermistor in order to record the air temperature during the testing program. Eq. 1 (see appendix) was used to correct the LVDT measurements. Moreover, strains and temperature in the pile were measured using twelve Vibrating Wire Strain Gauges (VWSGs) with integrated thermistors fixed at six levels along the pile shaft on two sides. The average of the temperature and strain measurements of the two gauges at each level was considered in the calculations, and their locations along the pile are shown in Fig. 1c. The length between each pair of strain gauges was termed a soil segment, with the soil compositions and dimensions of each segment shown in Table 1. The strain gauge measurements were corrected using Eq. 2 and then used to calculate the axial displacements along the pile shaft due to the thermo-mechanical load using Eq. 3 (see appendix). A ground source heat pump (GSHP) was connected to the pile (to extract/inject the energy) and the tank (to dissipate the extracted energy). Through heating the tank, the pile experienced cooling and vice versa. This process was used throughout the testing program to provide thermal load. The GSHP system employed a heat exchange fluid consisting of a precisely calibrated mixture of 30% monoethylene glycol and 70% water by volume. The flow rate during the cooling–natural heating was maintained at 7 l/min. Direct measurements were recorded at one-minute intervals, ensuring a consistent data collection.

The subsurface soil conditions at the project site were explored with a series of in situ tests, including cone penetration tests (CPTs). The results of CPT tip resistance (qc) are shown in Fig. 1d. Within the boring depth of 12 m, the subsurface soil comprised made ground, peat, silty sand, clay, and sand, Fig. 1c. Figure 1d shows that the soil strength (i.e., CPT tip resistance) is generally soft and weak soils. The weakest soil layers were peat and clay with CPT tip resistances of 0.3 and 0.8 MPa, respectively. The expanded pile tip was in sandy soil with tip resistance values of 6–10 MPa (Fig. 1e).

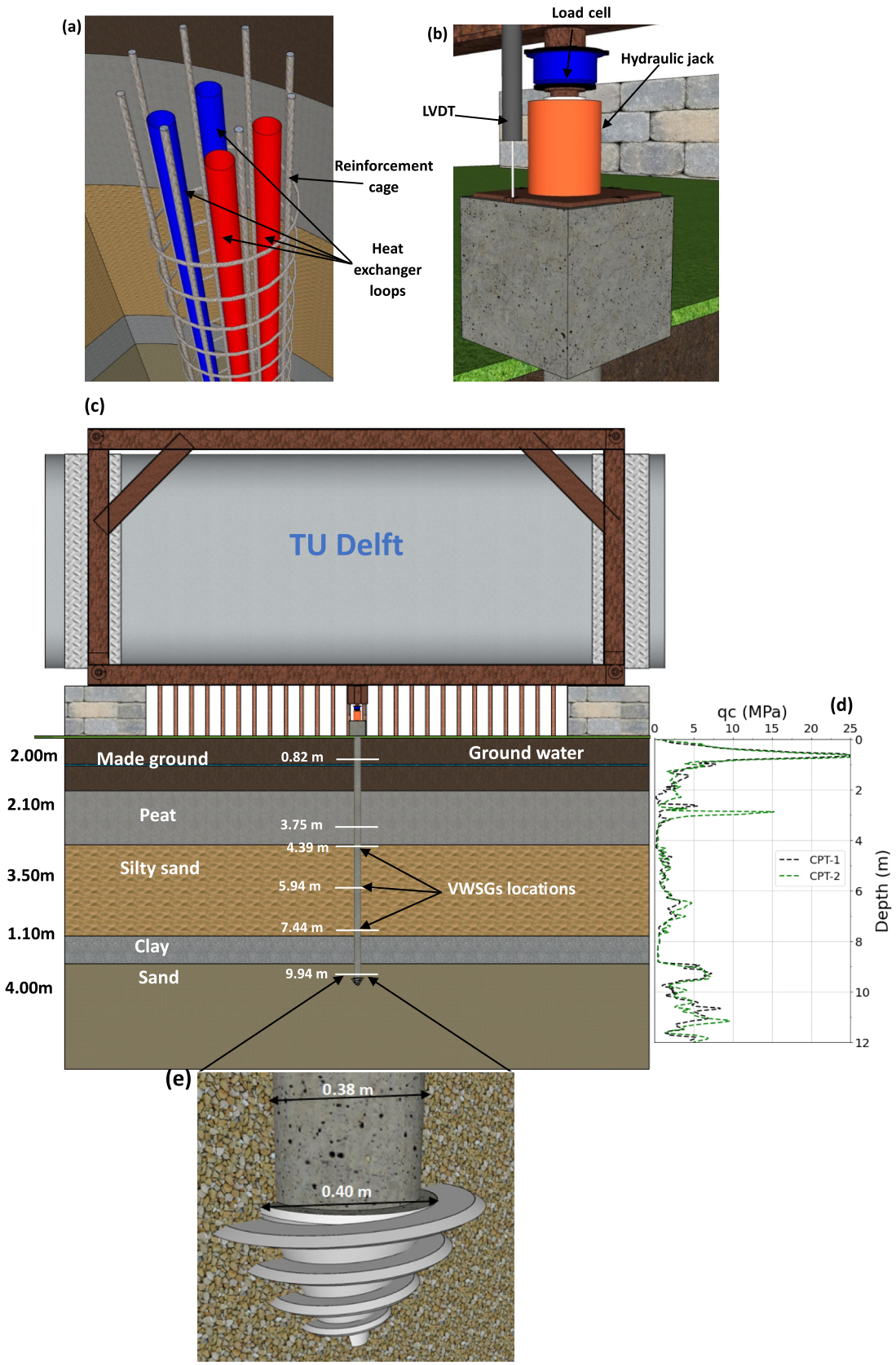

Fig. 1 Schematics of the energy pile: **a** reinforcement cage with the heat exchanger loops; **b** locations of LVDT, hydraulic jack, and load cell; **c** soil profile of the energy pile construction site with locations of VWSGs; **d** the results of CPT: cone resistances (qc); **e** sacrificial auger

Table 1 Dimensions and compositions of the soil segments

Soil segment	Location from the top of the pile (m)	Soil layers
Segment A	0–0.82	Made ground
Segment B	0.82–3.75	Made ground–peat
Segment C	3.75–4.39	Peat–silty sand
Segment D	4.39–5.94	Silty sand–silty sand
Segment E	5.94–7.44	Silty sand–silty sand
Segment F	7.44–9.94	Silty sand–clay–sand

3 Experimental scheme

The test program was conducted on a stand-alone energy pile over approximately two months (from Jul. 1, 2023, to Aug 31, 2023). It comprised two pure mechanical load tests without circulating fluid in the pile, a thermal test (without mechanical load), and three extended periods of thermo-mechanical testing. The testing program is presented in Table 2.

The two mechanical tests T_M1 and T_M2 were conducted before and after the thermo-mechanical tests, respectively, to investigate the effects of thermal cycles on the bearing capacity. In these two mechanical tests, the pile was loaded up to 60% of the estimated bearing capacity with increments of 10%. The Dutch code for static axial loading of piles with creep controlled to be less than 0.75mm/15min was adopted [47]. The pile bearing capacity was calculated to be 353 kN. Further details on the design of conventional piles using CPT data in the Netherlands are provided by Gavin et al. [18]. A free expansion test, T_0, was then conducted with no load applied to the pile. In this test, two cooling–natural heating thermal cycles were applied. In the thermo-mechanical stage, the pile was first loaded up to a specific target (30%, 40%, or 60% of the pile bearing capacity), inducing mechanical displacements along the pile. The applied mechanical load was held constant for a duration ranging from 10 to 16 h to reduce the creep effects; then, the pile was subjected to up to ten thermal cycles. The increasing loading scheme was chosen to ensure that the proceeding test did not impact the results of the following test. Using the same pile reduces the influence of local geotechnical and installations differences, thereby providing more quantitatively comparative results. To define the thermally induced axial displacement, the ongoing effect of the mechanical loading was considered to be negligible (negligible mechanical creep due to load applied to the pile head over time). Once the target temperature was reached, it was kept constant for 12 h, with an average applied temperature cooling of approximately 10 °C along the pile. This duration was determined by monitoring the temperature and stress change in the pile; when the stress reduction of the pile started (after approximately 2 h or less), it was assumed to be caused by the reaction of the ground. The cooling duration was then defined to be 12 h, ensuring an adequate cooling of the soil–structure interface. The air temperature at the Delft University of Technology site ranged from 30 °C to 7°C during the test period. The undisturbed ground temperature was approximately 12°C below a depth of 4 m. To simulate the realistic daily energy pile demand in the Netherlands, cooling–natural heating tests were conducted (cooling the pile and heating the building) while the mechanical load was held constant.

Table 2 Test program

Test No	Mode	Cycle	Cooling/natural heating duration (h)	Static load (kN)
T_M1	Mechanical	–	–	0, 36, 71, 106, 141, 176, 211
T_0	Thermal	2	12/12	0
T_30	Mechanical + thermal	6	12/12	106
T_40	Mechanical + thermal	10	12/12	141
T_60	Mechanical + thermal	10	12/12	211
T_M2	Mechanical	–	–	0, 36, 71, 106, 141, 176, 211

4 Full-scale in situ test results

The mechanical, monotonic cooling, and cyclic cooling–natural heating results of the pile displacements are presented. The post-processing of the recorded data is detailed in Appendix 1.

4.1 Mechanical behavior with no heating or cooling

Figure 2a and b presents the curves of pile head displacement versus the applied load and the mechanical axial displacement profiles, respectively, obtained from the static load tests T_M1 and T_M2. The results are nearly identical for 10, 20, 30, 40, and 50% of the estimated bearing capacity in each test, while under 60% the pile head displacement decreased significantly after thermo-mechanical

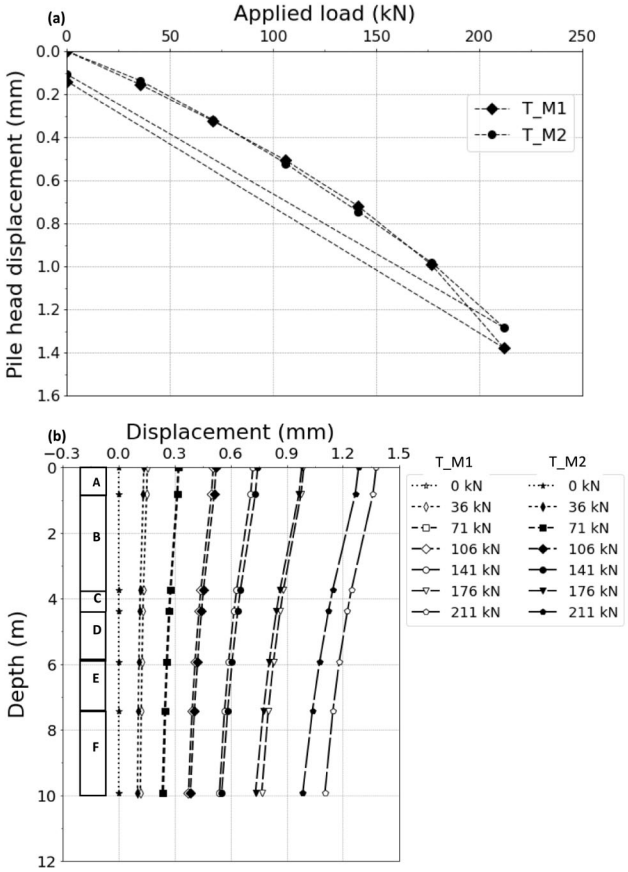

Fig. 2 Pile displacement of tests T_M1 and T_M2 under multiple mechanical conditions: **a** pile head load versus displacement curves; **b** mechanical axial displacement profiles versus depth at each segment

tests (i.e., T_M2). The pile head displacements under 60% of the estimated bearing capacity are 1.379 and 1.2852 mm in the tests T_M1 and T_M2, respectively, corresponding to 0.36% (T_M1) and 0.34% (T_M2) of the pile diameter. The application of thermal cycles to the pile therefore increased the bearing capacity. After unloading the pile in both tests, the results of the pile head displacements due to the mechanical loads (Fig. 2a) reveal an irreversible pile head displacement of 0.1404 mm and 0.1077 mm in the tests T_M1 and T_M2, respectively, corresponding to only 0.036% (T_M1) and 0.028% (T_M2) of the pile diameter. As seen in Fig. 2b, in both tests, the axial displacement relative (calculated from strain data using Eq. 3) to the soil decreases with depth. The ratios of the pile head displacement and the displacement in the last segment (immediately above the pile tip), as shown in Fig. 2b, are 0.93 and 0.89 for tests T_M2 and T_M1, respectively, indicating that the pile tip response is stiffer in the last segment.

4.2 Thermo-mechanical behavior under monotonic cooling

To investigate the axial displacement variation during a monotonic cooling phase in all tests, the results of the measured pile temperature, the computed corresponding thermally induced relative axial displacements, and static loading and cooling-induced axial displacements, after two different given moments (5 and 10 h of cooling) of the four tests are shown in Fig. 3a, b, and c, respectively. These two given moments are indicated in Fig. 4.

In Fig. 3a, the temperature profiles are shown. In test T_0, nearly a 2 °C difference between the upper part (from the top of the pile to 4.39 m) and the lower part (from 4.39 to 9.99 m) of the pile is observed, due to the higher initial temperature in the upper part. In addition, a slightly larger temperature change at around 4.39 m (see the temperature profile of the test T_0) is likely due to the annual thermal heat evolution, while in the other tests, the difference between the upper and lower parts of the pile became lower compared to the initial test 'T_0' with a lower temperature

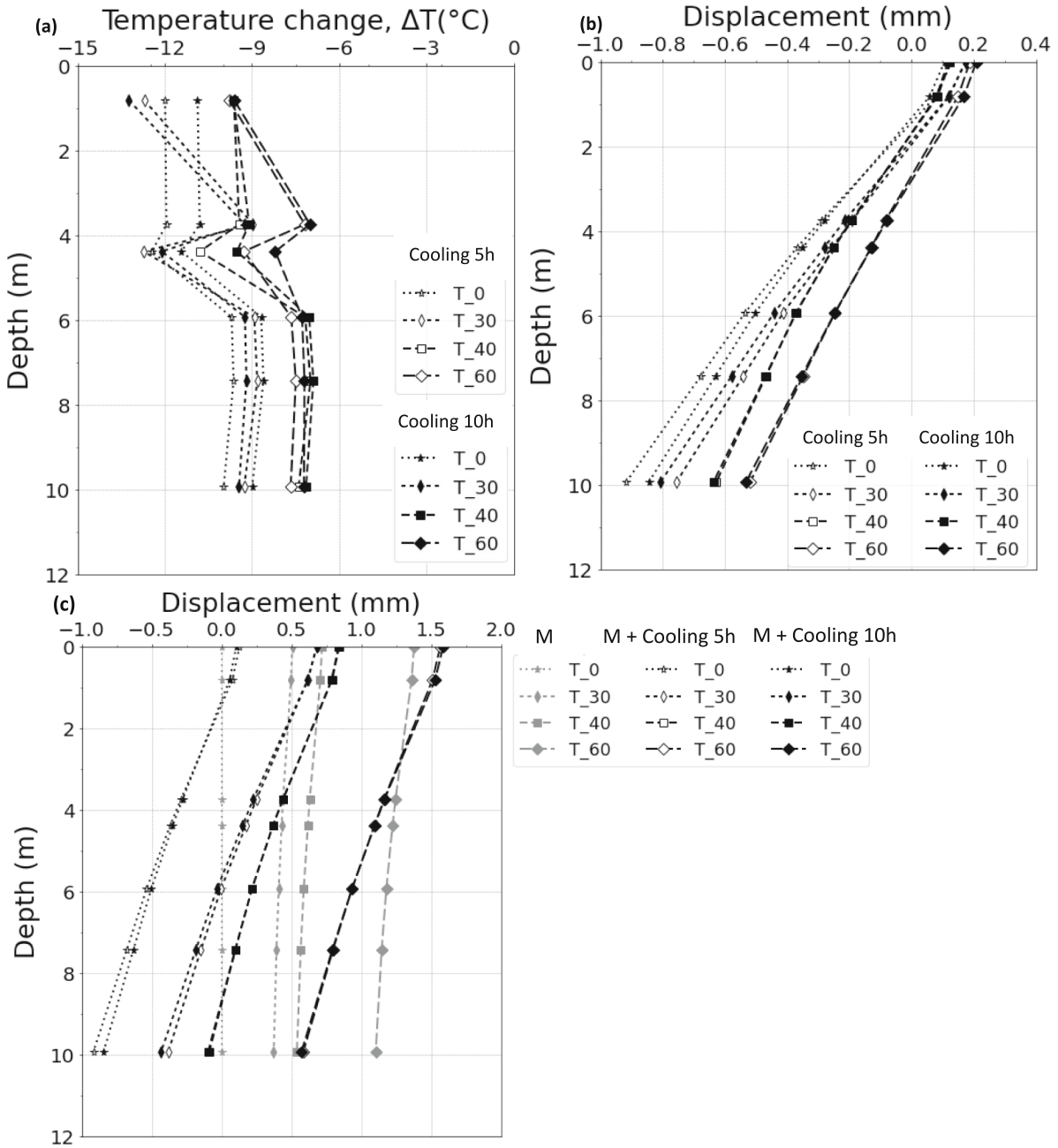

Fig. 3 Thermo-mechanical response of energy pile after 5 and 10 h of cooling obtained from the four conducted tests (T_0, T_30, T_40, and T_60): **a** measured pile temperature; **b** thermally induced axial displacement profiles; **c** mechanical (M) and thermo-mechanical axial displacement profiles after 5h (M + cooling 5h) and 10 h of cooling (M + cooling 10h) versus depth

change at around Level 2 (3.75 m), especially in tests T_30, which is likely due to the low thermal conductivity of the peat. The temperatures are shown at both 5 and 10 h after cooling. In all cases, the temperature change from 5 to 10 h was changed slightly (decreasing in tests T_0, T_40, and T_60, while in test T_30 slightly increasing) with a temperature variation of up to approximately (±1°C) from 5 to 10 h. In Fig. 3b, the axial relative displacement profiles along the pile, obtained after 5 and 10 h, reflect the changes in axial displacement due to the applied cooling. During the cooling phase, when the pile temperature decreases, contraction occurs that induces a settlement of the pile head and a relative uplift of the pile tip in all tests, as shown in Fig. 3b. In the free expansion test, after 5 h of cooling, the pile head displacement increased (i.e., settled), and in the lower part of the pile, from about 1m below the pile head to the bottom, the displacement decreased (i.e., uplift). Further cooling (i.e., after 10 h) led

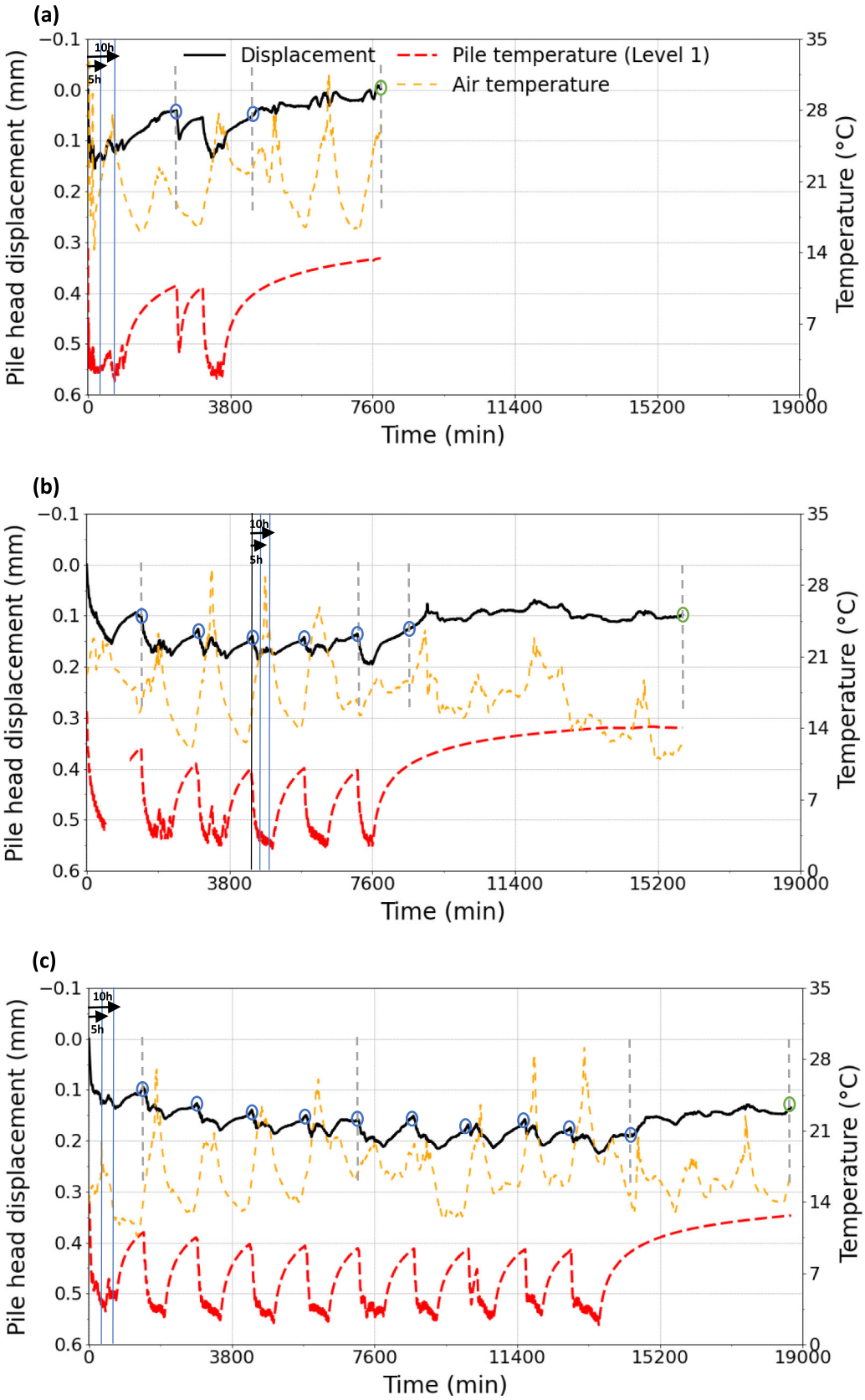

Fig. 4 Pile head displacement, air, and pile temperature variation (measured at the top of the pile) versus elapsed time of tests: **a** T_0, **b** T_30, **c** T_40, and **d** T_60

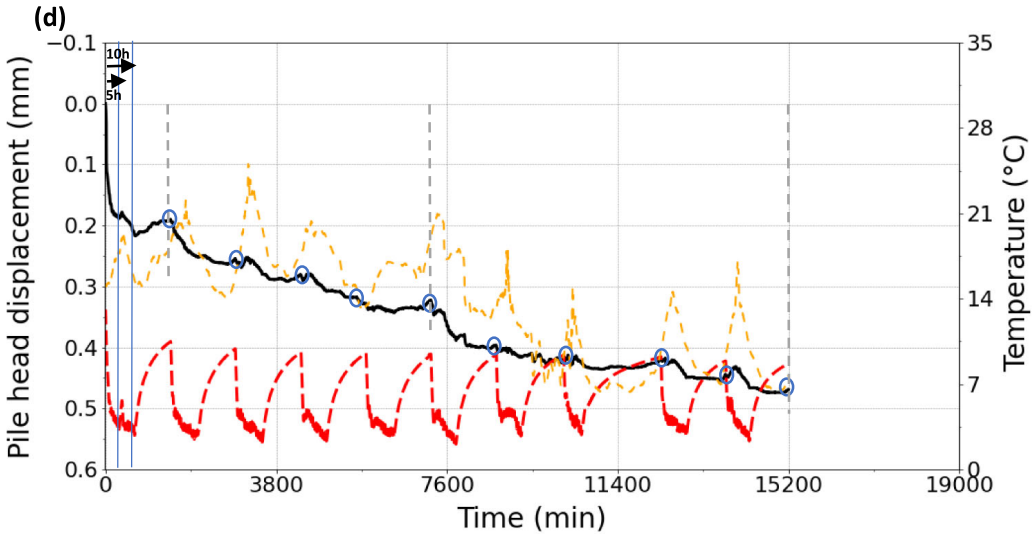

Fig. 4 continued

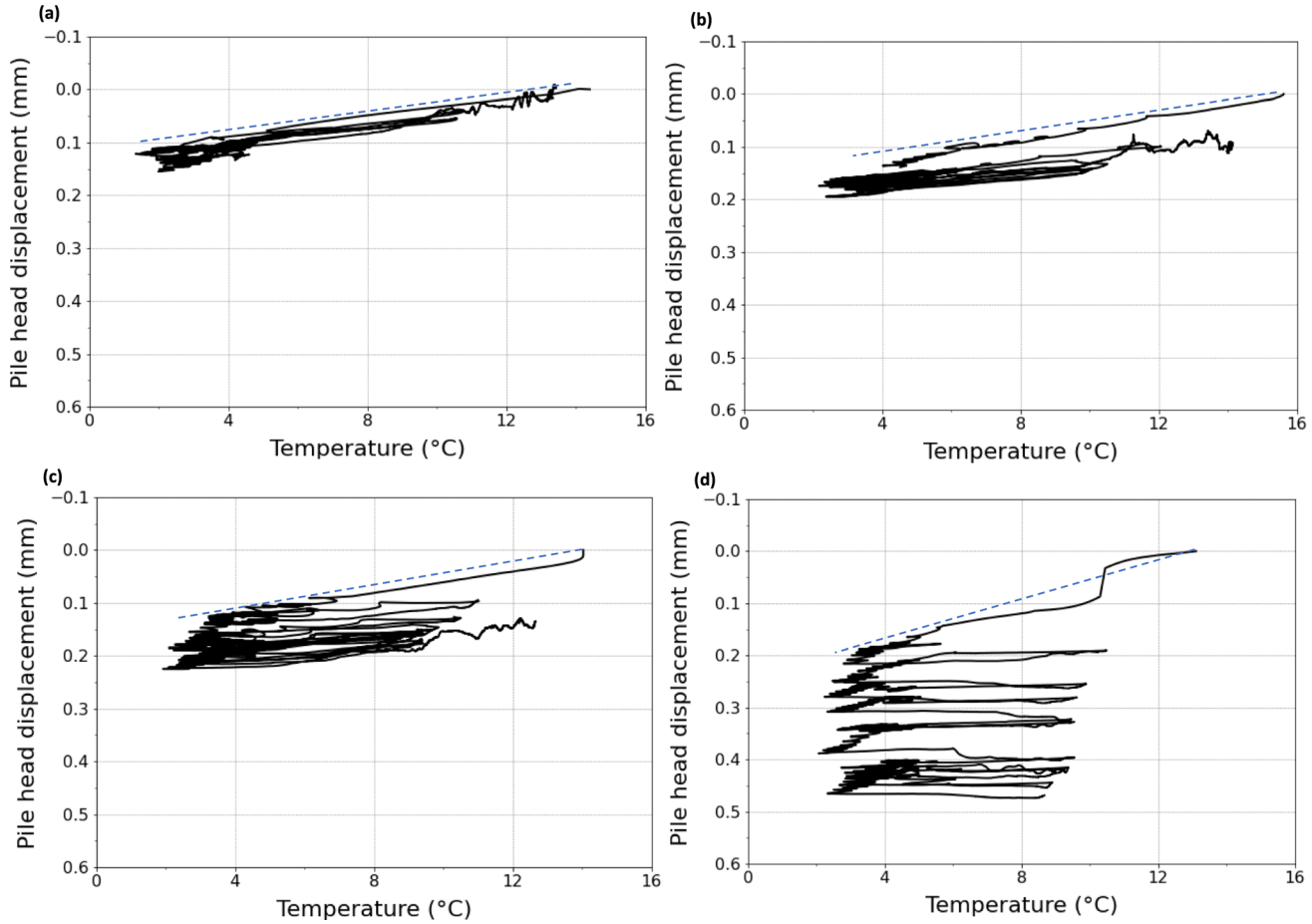

Fig. 5 Pile head displacement versus pile temperature of tests: **a** T_0, **b** T_30, **c** T_40, and **d** T_60

to a reduction in both the pile head settlement and the uplift in the lower part of the pile. This is consistent with a reduction in the temperature change, which was reasonably uniform along the pile (and the largest in this test). However, the relative displacement along the pile was not uniform and a higher reduction can be observed in the last

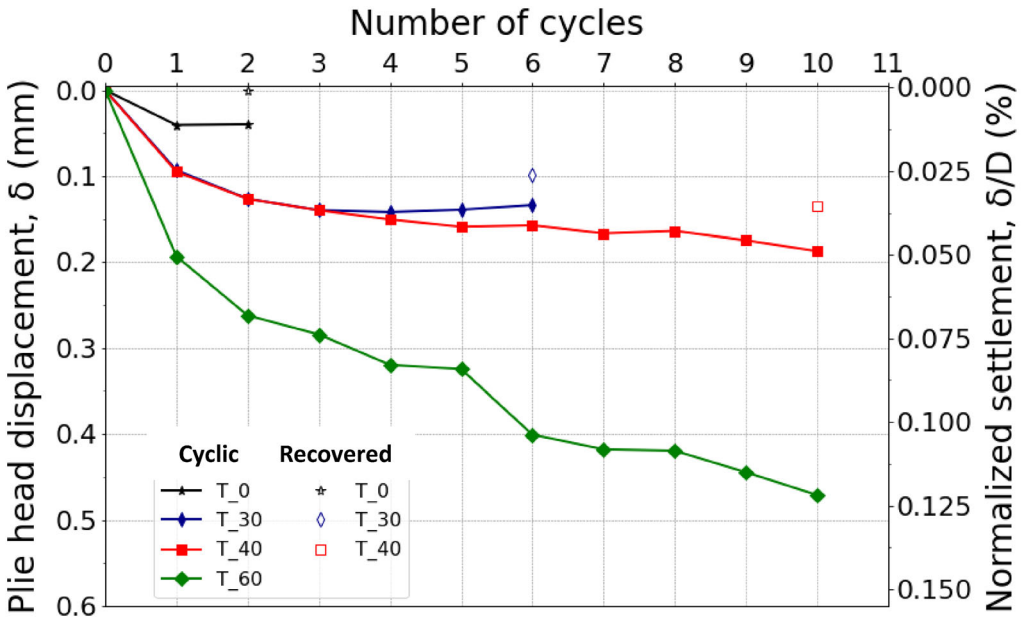

Fig. 6 Pile head displacement versus number of thermal cycles

segment next to the pile tip. In the other tests, T_30, T_40, and T_60, the pile head settlement and the uplift of the segment near the pile tip slightly increased from 5 to 10 h of cooling. These are consistent with more constant temperature change in the tests and a cooling of the soil surrounding the pile. It should be noted that the highest pile head settlement and the lowest uplift of segment F near the pile tip were observed in the test T_60 when the pile was under the highest mechanical load, while the lowest pile head settlement and the highest uplift of segment F near were noted in test T_0, although the temperature change was higher in test T_0 compared to T_60. However, under moderate mechanical loads (30 and 40%), the pile head settlement and the uplift of segment F near the pile tip were higher in test T_30 compared to T_40, following the magnitude of temperature change (see Fig. 3a). The thermal axial displacements induced by the cooling load were added to the mechanical axial displacements due to the applied mechanical load and are shown in Fig. 3c. The cooling load increased the pile head displacement and the axial settlement in the first segment A in all four tests. Additionally, it generated a net uplift near the pile tip in the other tests T_0, T_30, and T_40, while in test T_60 it reduced the net settlement that was initially induced due to the applied mechanical load. The changes in the axial pile displacements are dependent on the applied mechanical load. The neutral axis of the pile (where the combined temperature-induced and mechanical displacement line crosses the mechanical displacement line in Fig. 3c) is lower in the pile, and the slope of the thermally induced displacement against depth is lower with increasing load.

4.3 Thermo-mechanical behavior under cyclic cooling-natural heating loads

Pile head displacements, along with the air and the pile temperature measured by the LVDT and gauges at the base of Segment A (termed Level 1), respectively, versus elapsed time, are shown in Fig. 4a, b, c, and d for tests T_0, T_30, T_40, and T_60, respectively, during the thermal cycles. These figures reflect the changes in pile head displacement due to the applied thermal load. In Fig. 5a, b, c, and d, the pile head settlement is plotted versus the pile temperature change during the cooling–natural heating cycles for tests T_0, T_30, T_40, and T_60, respectively. These figures (Figs. 4 and 5) illustrate the pile thermal behavior under different degrees of freedom. During the first cooling phase (when temperature decreased), the pile settled in all tests. The subsequent natural increase in pile temperature during natural heating caused an uplift in all tests. In the free expansion test (T_0), the results reveal a large pile head uplift during natural heating (i.e., in the first thermal cycle), and reversible pile head displacement was observed when the temperature was restored in the second thermal cycle (Fig. 4a). The relationship between the pile head settlement and the pile temperature is linear, following the pile thermal expansion curve (Fig. 5a). In thermo-mechanical tests (T_30, T_40, and T_60), similarly the pile head settled during the first cooling phase, with higher settlements observed under higher mechanical loads with respect to the temperature variation. The subsequent natural increase in pile temperature during natural heating led to uplift but did not retrieve the settlement, i.e., was

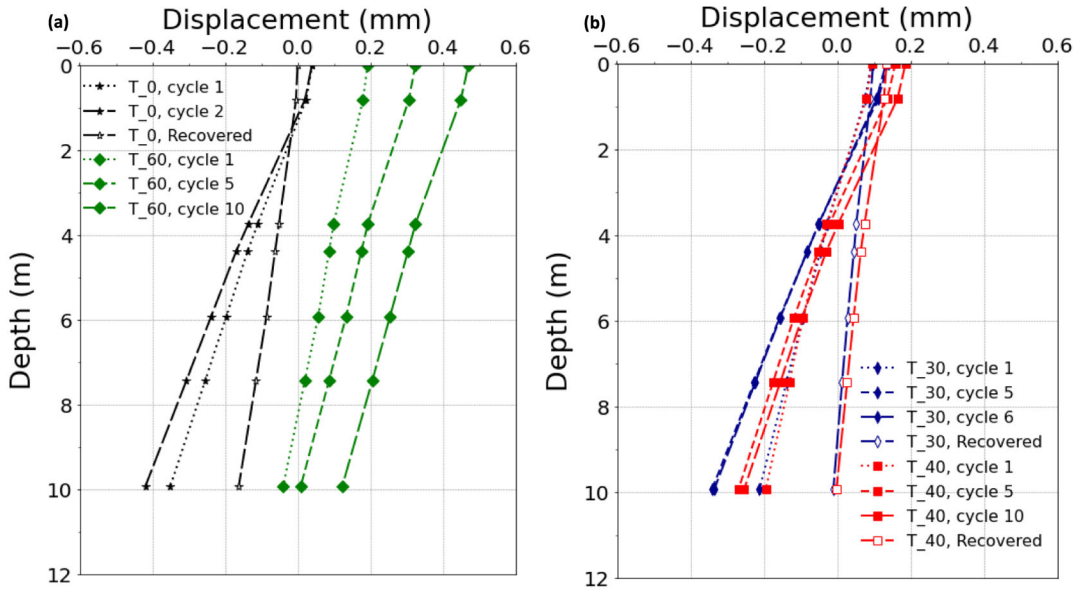

Fig. 7 Thermally induced pile displacement evolution versus depth for tests: **a** T_0 and T_60; **b** T_40, and T_40

permanent. This trend was consistent throughout test T_60 and only in the first three and four thermal cycles in tests T_30 and T_40, respectively. In these tests (T_30 and T_40), nearly similar magnitudes of settlement and uplift of the pile head were observed in the subsequent cycles (after the first four thermal cycles), following the magnitude of temperature change. In Figs. 4d and 5d, the displacement tracks the temperature change in the pile less well than the other tests, probably indicating that it is linked to ratcheting effects of the pile–soil interface due to thermal cycles under constant mechanical load as observed in laboratory experiments by Rafai et al. [53], rather than thermally induced mechanical cycles on the pile–soil interface due to pile contraction–expansion, following the decrease–increase in pile temperature. Note also that during the cycles the temperature drops slightly (see Fig. 4) and after the last cycle is allowed to relatively recover in tests T_0, T_30, and T_40 with a maximum of 1 C° of residual temperature difference, which allows the permanent displacement to be assessed. The pile head uplift during natural heating is dependent on the applied mechanical load and is lower under higher mechanical loads. Figure 5a, b, c, and d shows that the slope inclination (indicated by dashed blue lines) of the first cooling phase is steeper under higher mechanical loads compared to under lower mechanical loads. This indicates a major impact of the applied mechanical load on pile settlements.

In Fig. 6, the irreversible pile head settlement and its ratio to the pile diameter (normalized settlement) at the end of each cycle and after thermal recovery (with a maximum of 1°C of residual temperature difference at level 1, see the blue and green circles in Fig. 4 for the time the cycle is considered to have ended and recovered, respectively) are plotted versus the number of thermal cycles for all four tests. When the pile was free of load, an irreversible settlement of 0.05 mm was observed at the end of the first thermal cycle, while at the end of the test, it was negligible, nearly zero. In the other tests, the higher the pile head load, the more significant the observed settlement. After the first cycle of these tests, irreversible pile head displacements of 0.09 and 0.095 mm were observed in the tests T_30 and T_40, respectively, which were closely similar. In the test T_60, 0.2 mm of settlement was observed. In tests with mechanical loads, the irreversible settlement consistently increased with each cycle, while the rate of accumulated settlement decreased with increasing cycle numbers. This rate tended to stabilize after three thermal cycles in test T_30 and four thermal cycles in test T_40, noting that the observed settlement in these tests during the first three thermal cycles was nearly similar. However, in the test T_60, the rate of the irreversible settlement did not stabilize, and it continued to increase at a slightly reduced rate over the 10 applied thermal cycles. Furthermore, for the same thermal cycle, pile head displacement was higher under a higher mechanical load. In the four tests, the largest displacements were observed after the first cycle. The observed irreversible settlement at the end of tests T_0 (recovered), T_30 (recovered), T_40 (recovered), and T_60 was approximately 0, 0.1, 0.142, and 0.471 mm, respectively.

The evolution of thermally induced pile displacement versus depth is presented in Fig. 7a for T_0 and T_60, while in Fig. 7b for tests, T_30 and T_40, for different

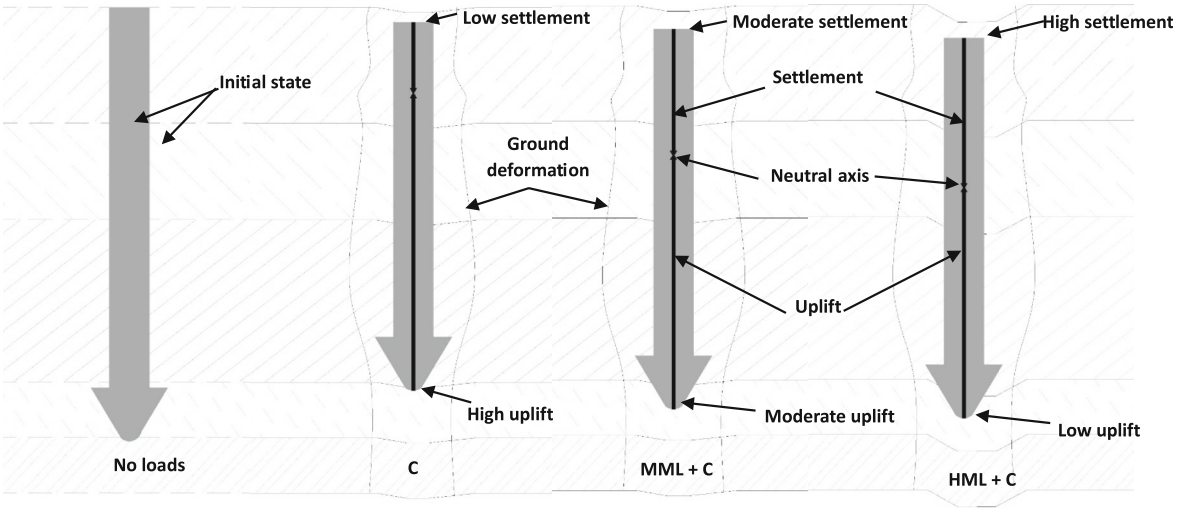

Fig. 8 Pile response during monotonic cooling (c) under zero mechanical load, moderate mechanical load (MML), and high mechanical load (HML)

number of thermal cycles for each test (see the dashed gray lines in Fig. 4).

Under no mechanical load in test T_0, after the first thermal cycle, a settlement of the pile head and along the segment A was observed while uplift was noted in the other segments. After the second cycle, the settlement of the pile head and along segment A remained constant, while an increase in the observed uplift was noted in the other segments. At the end of this test, the settlement of the pile head and in segment A was negligible, while a permanent uplift was observed in the other segments after the pile temperature had recovered to virtually the initial temperature. This indicates a redistribution of thermally induced stresses, with no surface settlement or strain near the pile head.

Under higher mechanical load in test T_60, uplift was observed only after the first thermal cycle in the last segment F, while axial pile settlement was noted in the other segments.

The difference in the magnitude of pile head and segment A displacements between 1 and 5 cycles was the highest in the pile, with the difference reducing with depth. However, there was a closely similar magnitude of the axial settlement along the pile between 5 and 10 thermal cycles. This perhaps indicates a change in process, from being initially dominated by dragdown of the surrounding soil, i.e., the impact of ground shrinkage, due to the transfer of cooling-induced load and moving toward accelerated rates of thermally induced ratcheting at the pile–soil interface and compaction of the sand beneath the pile tip. Further details are discussed in the discussion section.

Under moderate mechanical load in tests T_30 and T_40, after one thermal cycle, the pile head settlement and the axial displacement in segments A, B, C, and D were nearly similar, while in segments E and F, a slightly higher uplift was observed in test T_30 compared to T_40. In both tests, after 5 thermal cycles, the pile head settlement and the axial settlement in segments A and B slightly increased while the uplift slightly increased in the other segments. After 6 and 10 thermal cycles in tests T_30 and T_40, respectively, the pile head settlement and the axial settlement in segments A and B slightly increased while the uplift slightly decreased in the other segments. At the end of these two tests, when the pile temperature had almost recovered, permanent axial settlement was observed along the pile except in segment F, near the pile tip, a nearly negligible settlement was observed. The magnitude of the observed axial displacement along the pile was higher in the test T_40 compared to T_30. The gradient of this permanent thermally induced displacement is similar between tests T_30 and T_40, indicating the pile had settled almost uniformly along its length, indicating a nearly similar amount of permanent thermally induced axial stress (and therefore also mobilized shear strength).

The neutral axis is dependent on the applied mechanical load and the number of cycles. At the maximum number of cycles in test T_0, it was near the pile top; in tests T_30 and T_40 it appeared around mid-pile and in test T_60 below the pile.

5 Discussion

This research focused on the effect of coupling heat exchange and multiple mechanical load levels on the mechanical responses of the pile, as well as the impact of the thermal cycles on the pile bearing capacity.

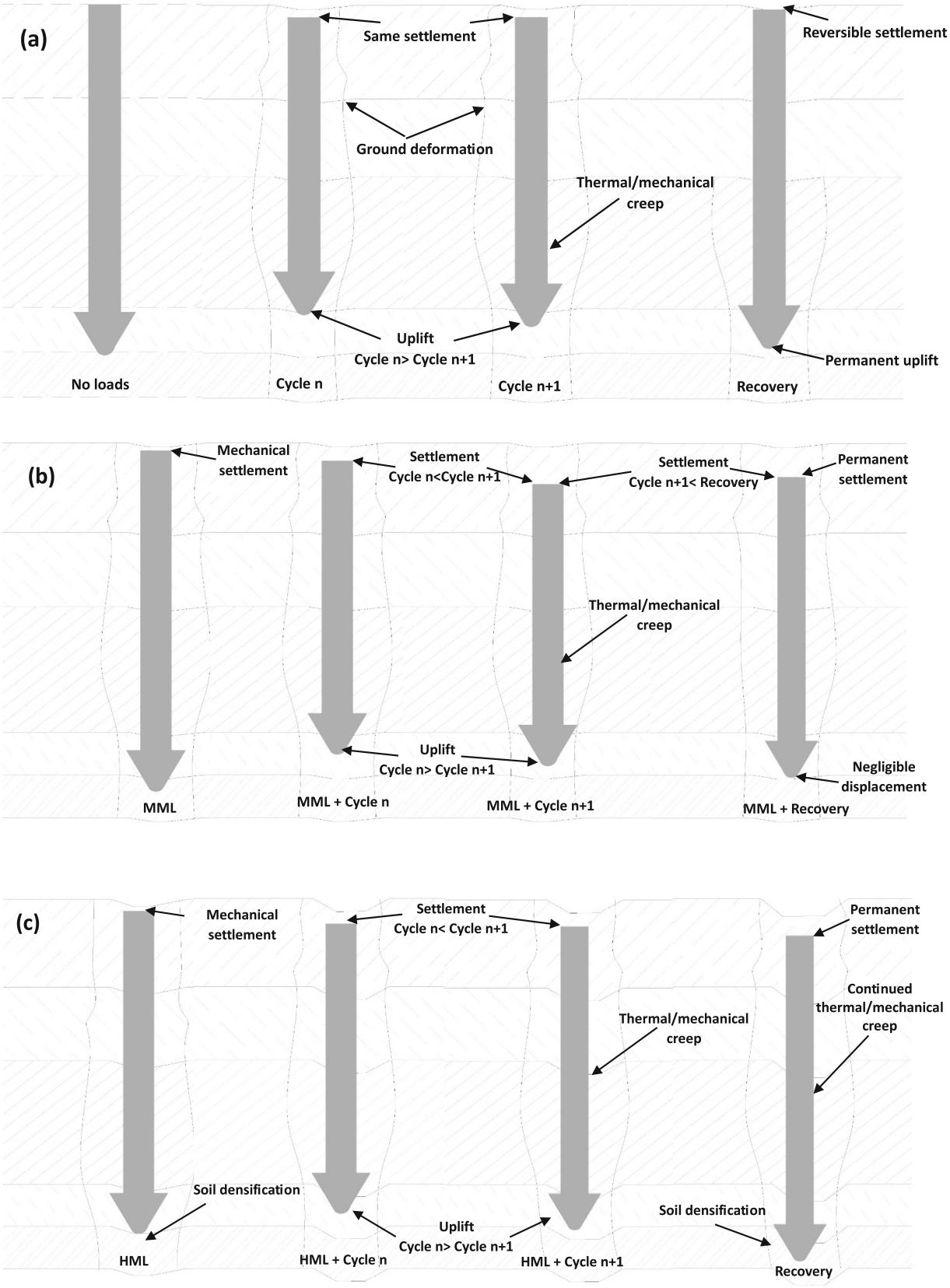

Fig. 9 Pile response after cooling–natural heating thermal cycles under **a** zero mechanical load, **b** moderate mechanical load (MML), and **c** high mechanical load (HML)

In the monotonic results, the decrease in the axial relative displacement (both the settlement and the uplift) of the pile from 5 to 10 h of cooling in the test (T_0) can be partially attributed to the decrease in the temperature variation and partially due to the successive dragdown of the subsurface due to the applied cooling load (Fig. 3b). The time-dependent phenomenon of transferring the cooling-induced load to the near soil depending on the temperature magnitude and the initial stress state could lead to different magnitudes of the shrinkage of the surrounding soil and sand beneath the pile tip and thus different dragdown magnitudes. This dragdown effect was also manifested as a reduction in cooling-induced tensile stress by Rafai et al. [52]. A higher tensile stress reduction over time was observed when the pile head was under a larger applied mechanical load, which may reduce the displacement along the pile relative to the soil and thus reduce the confining pressure [25, 52]. Therefore, there is greater additional axial pile settlement, especially in test T_60 (Fig. 3c). Moreover, a potential mechanical creep along with the slight temperature variation along the pile could result in an increase in axial settlement near the pile head and a slight increase in the uplift of the segment F near the pile tip in tests T_30, T_40, and T_60, from 5 to 10 h of cooling (Fig. 3b). A similar trend was reported by Gawecka et al. [19] where the stress was observed to reduce with time as the surrounding soil reacted to the changes imposed on the pile.

In the test (T_0), the observed settlement of the pile head and segment A as well as the uplift of the other segments after the first thermal cycle can be explained by the pile temperature not being completely restored (Fig. 7a). However, the observed increment in the uplift near the pile tip (while the displacement of the pile head and segment A remained unchanged) after the second cycle could be explained by the larger expansion (i.e., the total reduction in the net contraction) of the ground during the natural heating compared to the expansion (i.e., the total reduction in the net contraction), of the pile as the ground temperature should be higher than the pile during natural heating (heat (cold) from the soil (pile) to the pile (soil)), or plastic yield at the lowest point. At the end of this test, when the temperature was fully restored (after thermal recovery with about less than 1 C° of low residual temperature), the pile head displacement was zero and generally appeared to be perfectly thermo-elastic, as linear and reversible pile head behavior was observed (Fig. 5a). However, permanent uplift was observed in the lower part of the pile, which can be explained either by the larger uplift of the surrounding soil compared to the downward settlement of the lower part of the pile during natural heating, or the successive dragdown of the surrounding soil layers that could happen during this test would induce a higher force at the lower part of the pile, or both. In both cases, the ground would reduce and restrict the potential settlement of segments E and F near the pile tip (i.e., the total reduction in the net uplift, recovery to the initial state) and thus an apparent permanent uplift of the pile. These observations imply a presence of residual stress, especially in segments E and F at the end of this test, even though heating (i.e., higher temperature than the initial one) was not applied.

Under moderate mechanical load, in tests T_30 and T_40, the irreversible settlement during the first 3 and 4 thermal cycles, respectively, can be partially attributed to the low residual temperature in the pile and soil and partially to the dragdown effect of the soil. The observed similarity in the first 3 thermal cycles in these tests (see Fig. 6) can be attributed to the higher unrecovered temperature in test T_30, indicating a steeper downward trend due to the low residual temperature compared to T_40 (see Fig. 4b, c), while the impact of the applied mechanical load is clearly shown in the slope in Fig. 5b, c. When the temperature was recovered, the pile head displacement partially recovered. These results slightly align with those reported by Faizal et al. [13] where a reversible thermal response at the pile–soil interface was observed for an energy pile subjected to thermal cycles under 52% of the estimated ultimate load.

In these two tests, the uplift of segments E and F increased from 1 to 5 thermal cycles, while the pile head settlement slightly increased (see Fig. 7b), possibly due to the unrecovered temperature. As stated previously, the time and magnitude difference of the uplift of the soil and pile could also contribute to this increase of the observed uplift near the pile tip, as the pile contracts (expands) before (after) the contraction (expansion) of the surrounding soil during cooling (natural heating). From 5 to 6 and from 5 to 10 thermal cycles in test T_30 and T_40, respectively, the pile head settlement slightly increased while the uplift of

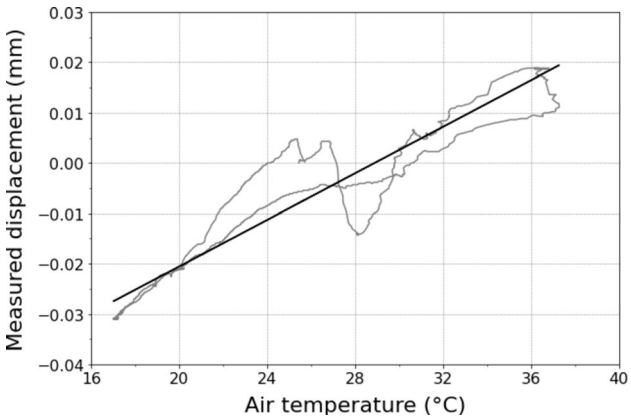

Fig. 10 Calibration test: Measured displacement versus air temperature (prior to the test)

segment F slightly decreased, indicating a downward settlement along the pile, although the temperature magnitudes were nearly similar in these cycles in each test, probably due to dragdown of the surrounding soils and the contraction of sand beneath the pile tip. This can be attributed partially due to the accumulated low-residual temperatures (not fully recovering during the cycles) and partially due to the accumulation of the inherent thermally induced irreversible deformation of the soil [4, 9, 10, 21, 37, 48, 49, 56]. After the temperatures had almost recovered, the displacements of the pile shifted from uplift to settlement, except near the pile tip where there was almost zero displacement, the settlement was nearly negligible. This indicates a thermal creep at the pile-soil interface. Under higher mechanical load (i.e. test T_60) a continuous accumulation of irreversible pile head displacement, in a ratcheting pattern at a reduced rate with an increasing number of cycles was observed (Fig. 6). This pattern behavior is similar to the findings reported by Yavari et al. [61], Ng et al. [43], Yavari et al. [62], Nguyen et al. [46], Ng et al. [45], Ng and Ma [40], and Kong et al. [25] exhibiting an irreversible settlement in the long-term, with thermal settlement being greater under higher constant head loads. This behavior is particularly critical in the case of floating energy piles, where irreversible ratcheting settlement has been observed [20, 45, 50, 64]). Previous studies (those above, and [44, 54, 55]) attributed this behavior to a decrease in the resistance of the pile-soil interface with an increasing number of thermal cycles. Fang et al. [16] reported a pile head displacement (i.e. pile A in energy piles group) of 1.13 mm after four heating natural cooling cycles, noting that the four piles were connected by a cubic cap and were under 440 kN of mechanical load. This value was relatively higher than the reported in this study which was 0.33 mm after four cooling natural heating cycles under 211 kN of mechanical load. It should be noted that the same energy pile exhibits different magnitudes of pile displacement depending on the applied mechanical loads and temperature variations. As stated previously, qualitative alignment with the existing literature is obvious while quantitatively, differences are expected, especially when comparing the results reported in this study with other studies (e.g. by Fang et al. [16]) in different ground conditions, and pile type and dimensions. This non-uniform behavior of energy pile and stresses redistribution has been reported numerically by Abdelaziz and Ozudogru [1]. Feng et al. [17] reported that cyclic thermal loading could alter the proportions of the mobilized shaft and tip resistances. This may contribute to plastic deformation under a higher mechanical load level.

The studies on soil-structure interfaces by Golchin et al. [20] and Rafai et al. [50] showed a shear displacement due to the thermal load in a ratcheting pattern. This thermal creep at the soil-structure interface was found to be larger in the case of loose soil [50], which is the case in this study, where the energy pile in soft soil was investigated. This may explain the observed irreversible settlements, especially in test T_60 from 5 cycles to the end of this test along with the contraction of sand beneath the pile tip, resulting in uniform settlement along the pile (i.e. see the difference between "T_60, cycle 5", and "T_60, cycle 10" near the pile top and tip in Fig. 7a). As stated by Rafai et al. [53], the thermally induced deformation of coarse-grained soils is less pronounced compared to fine-grained soils. Therefore, this accelerated ratcheting in test T_60 after 5 thermal cycles, is largely due to the dominant thermally induced ratcheting at the pile-soil interface and slightly due to the contraction of sand beneath the pile.

Another possible reason that might explain the lower uplift in thermomechanical tests and the observed settlement is the potential existence of mechanical creep deformation under a constant working load as also observed by Ng and Ma [40]. This could be significant under a higher mechanical load, for this reason lower uplift was observed under a larger mechanical load which implies a minor downward settlement due to the potential mechanical creep.

Ng et al. [42] and Kong et al. [25] observed permanent settlement of 0.56%D during monotonic heating and 0.59%D after three heating-natural cooling cycles, respectively. The observed permanent settlement was attributed mainly to the thermal contraction of the medium-dense sand during heating as a result of the large pores' thermal collapse which was larger than the thermal expansion of sand grain, illustrating the possible effect of thermal contraction of the surrounding sandy soil on the pile response permanent settlement.

Note that the higher the initial stress, the more susceptible soil is to the thermally induced contraction during cooling [2, 53] and the higher the thermal creep at the soil-structure interface is [7, 20, 50].

Ren et al. [55] reported that the application of a cooling load to the pile caused the shrinkage of the pile and reduced the soil pressure between the pile and the soil, and when the load acted on the pile head, the pile side friction resistance decreased. Thus, the displacement of the pile head was larger in the last mechanical test compared to the first one. However, while monotonic and cyclic thermal behavior were tested, their impact on the pile bearing capacity was not. In agreement with this observation, Luo et al. [31] explained that the increment of shaft resistance was due to the radial expansion during heating, while cooling decreased the radial stress at the pile–soil interface. There are few tests available on the bearing capacity changes due to temperature cycles. Liu et al. [29] noted a limited reduction in bearing capacity after up to 5 cycles,

whereas Wang et al. [59] indicated that no losses in pile shaft capacity after thermal loading cycles and suggested this was due to pore water viscosity in saturated soil which could have contributed to the swifter recovery of the pile-soil interface. However, Yazdani et al. [63] observed that piles subjected to heating-natural cooling exhibited greater shaft resistance than the reference pile tested at room temperature. In this testing program, the partial shaft degradation along two segments, A and D, due to the repeated cyclic shearing contraction/expansion at the soil-structure interface was observed by Rafai et al. [52], and the reduction in the pressure (even temporarily) at the soil-structure interface due to the lateral contraction of the pile and shrinkage of the surrounding soil induced an axial displacement at the pile-soil interface, especially under higher mechanical load. To compensate for both temporary and permanent shaft pressure reduction and thermal creep at the interface [20, 50], the load shifted from the shaft to the tip resistance (for equilibrium of axial load), leading to denser sand beneath the pile tip. Therefore, a lower displacement was observed in the last mechanical load, suggesting a stiffer/stronger behavior. This led to an additional pile capacity (Fig. 2a). Note that thermal cycles affected particularly segment A which is initially weak and is an unsaturated layer. Stress history (whether thermally induced, or otherwise) can impact the performance of a pile. Duffy et al. [12] retested axially loaded precast piles under 60% of the 'measured' pile capacity and an additional pile capacity was observed in both piles. This additional capacity is similar to the observed in this study on energy piles (note that in this study, the pile was loaded to 60% of the 'estimated' energy pile capacity). Both piles had undergone a mechanical stress history, which appeared to result in additional capacity. Likely due to the irreversible contraction of sand below the pile tip, which was observed as an irreversible pile head displacement after the first mechanical test, T_M1. Although this was small i.e. 0.1 mm (Fig. 2a), it could slightly contribute to the increase of tip resistance along with the thermally induced pile settlement of 0.47 mm in test T_60 (Fig. 6).

To summarize, it seems that until 40% of the pile capacity, the behavior of the pile remains mostly thermo-elastic after a limited number of thermal cycles. While an important thermo-plastic behavior was observed at 60% of the pile capacity. It is likely that either thermal creep and a redistribution of load to the pile tip or thermal creep at the pile-soil interface combined with the thermal collapse of the sand at the pile tip resulted in a denser sand below the pile tip and therefore higher tip resistance.

A conceptual schematic of the potential mechanism of the energy pile response during monotonic cooling under three states of mechanical loads, i.e., no mechanical load, moderate mechanical load, and high mechanical load, is presented in Fig. 8. The pile movements response appears to be driven by mainly four mechanisms of different magnitudes: First, the contraction of the pile itself from both ends toward the neutral axis, i.e., where the displacement is zero, due to the decrease in the pile temperature, which induces settlement of the upper part and uplift of the lower part. Second, mechanical and /or thermal creep, which might contribute to the higher pile head settlement and the lower uplift of the segment near the pile tip under moderate and higher mechanical loads. Third, the dragdown of the surrounding soil and compaction of soil beneath the pile tip. This may happen due to the transfer of the cooling-induced load to the near soil, leading to a reduction in the confining stress at the soil–structure interface and thus further settlement. The magnitude of the pile settlement would be dependent on the applied mechanical load. The thermal collapse of soil beneath the pile is unlikely during monotonic, especially under no mechanical load, as the pile head settlement is lower than the uplift of the segment near the pile tip when the pile is free. Fourth, the plasticity at the interface; this could happen when the pressure at the interface reduces either due to the repeated contraction/expansion shearing cycles, lateral pile contraction, or dragdown of the adjacent soil [53].

The potential mechanism of the energy pile response during cyclic cooling–natural heating under three states of mechanical loads, i.e., no mechanical load, moderate mechanical load, and high mechanical load is presented in Fig. 9a, b, and c, respectively. Under zero mechanical loads, after a certain number of cycles pile head settlement and the uplift of the lower part of the pile increased mainly due to the contraction of the pile as a result of the pile temperature reduction. Further thermal cycles, the pile head settlement may remain constant while the uplift of the pile tip decreases. This is mainly due to the low residual temperature in the soil and along the pile causing an elastic behavior along with a possible thermal plasticity of the surrounding soil, which could lead to a permanent uplift even after thermal recovery.

Under moderate mechanical loads, settlement at the pile head accumulates and an initial uplift is observed at the tip. After a certain number of cycles, pile head settlement becomes negligible and there is moderate uplift of the lower part of the pile, which then also stops. Further thermal cycles could cause further settlement along the pile at an increasingly slow rate. Mechanical and thermal creep as well as the dragdown of the subsurface could slightly contribute to the permanent settlement after thermal recovery.

Under high mechanical loads, both the pile head and pile tip settle. After a limited number of cycles, the pile head and tip continue to settle at a reduced rate, which seems to

continue unchanged. Further thermal cycles would cause further settlement along the entire pile, leading to densification of soil beneath the pile tip. This is likely due to the combined effects of the mechanical and thermal creep at the pile–soil interface. These effects are dependent on the applied mechanical loads. Further details on the applied mechanical load on the thermally induced contraction of sand and shear displacement of the sand–structure interface are elucidated by Rafai et al. [53].

6 Conclusions

A stand-alone energy pile was subjected to a sequence of pure mechanical loads, followed by a cooling-natural heating path (under zero mechanical load), then multiple mechanical loads (30%, 40% or 60%) coupled with thermal cycles (up to ten thermal cycles), and finally another mechanical load test identical to the first one to assess the effect of thermal cycles on the pile bearing capacity. The following conclusions can be drawn:

- Monotonic cooling load increased the pile head settlement in all four tests and induced an uplift in the segment near the pile tip. Larger pile head settlements and lower uplift were observed under higher mechanical load.
- Under zero mechanical load, thermal cycles induced fully reversible pile head displacement. However, a permanent uplift was observed near the pile tip at the end of this test. Under constant mechanical loads, thermal cycles induced an irreversible settlement of the pile head. This thermally induced vertical pile head displacement increased with the number of cycles. The rate of this increment was slower and stabilized under lower mechanical loads (30 and 40%), while under a higher mechanical load, i.e., 60%, continuous pile head displacement was observed with an increasing number of thermal cycles. The applied mechanical load was shown to be a key parameter that controls the thermally induced irreversible pile displacements.
- In the thermo-mechanical tests, a shift from the uplift of the segment near the pile tip to settlement was observed, leading to permanent axial settlement along the pile. This was largely the thermal creep of the soil–structure interface and the larger contraction of sand beneath the pile tip. This permanent axial settlement was higher under a higher mechanical load and was attributed to larger downward thermal creep at the pile–soil interface and contraction of the sand beneath the pile, mobilizing a greater toe resistance under a higher mechanical load.
- Additional pile capacity was observed after the thermo-mechanical tests and attributed to the irreversible settlements (due to the mechanical and thermo-mechanical loads) which densified sand beneath the pile, leading to higher tip resistance. The degradation of shaft resistance was negligible compared to the increase in the pile capacity and could be compensated by the tip resistance.
- This study indicates that the pile settlement caused by cyclic thermal loading can be acceptable for general engineering structures, with no exceedance observed, and can even increase pile capacities. Nonetheless, thermally induced pile settlement should be cautiously considered, especially under higher mechanical loads.

Appendix

Calibration and processing of the in situ test data

The relationship between the measured vertical displacement and air temperature prior to conducting thermal cycles is presented in Fig. 10. The strain along the pile during this phase remained constant; therefore, this effect was considered to be an impact on the displacement measurements due to the air temperature. The obtained results were fitted using linear regression:

$$D = 0.00231T \tag{1}$$

where D is vertical displacement (mm) and T is air temperature (°C). Equation (1) is used to calibrate the measured vertical displacements of the pile and was applied to all conducted tests.

The strain data along the test pile were recorded by VWSGs. The strain gauges also expand with temperature. The strain of the pile, i.e., the measured strain, was calculated from the gauge readings using the following equation:

$$\varepsilon_{\text{meseared}} = \varepsilon_{\text{gauge}} + \alpha_{\text{gauge}}\Delta\text{T} \tag{2}$$

where α_{gauge} is the coefficient of linear thermal expansion of the steel wire in the gauges (11 με/°C) and ΔT is the temperature change of the pile. At the start of the thermal tests, the gauge strains along the pile ($\varepsilon_{\text{gauge}}$) were zeroed, and then, Eq. (2) is used to correct the results.

The displacement (δ_i) at any point along the pile can be calculated as follows:

$$\delta_i = \delta_{i-1} - \frac{1}{2}(\varepsilon_{i-1} + \varepsilon_i)\Delta l \tag{3}$$

where Δl denotes the distance between strain gauges i and i-1. Note that in this study the positive displacements indicate settlement.

Acknowledgements Part of the work presented was carried out within the scope of the following projects: Netherlands Organisation for Scientific Research (NWO) project number 14698 "Energy Piles in the Netherlands"; COST Action CA21156 "European network for FOstering Large-scale ImplementAtion of energy Geostructure (FOLIAGE)"; PRIN2022 "Closing knowledge gaps on energy geostructures for retrofitting of buildings and infrastructures (GEOREFIT)"; CETP22FP-2022–00147 "Large-scale climate neutral Energy Geostructures in District Heating & Cooling systems/networks (LEG-DHC)"; the first author was partially supported by ERASMUS+.

Author Contribution First author (Mouadh Rafai) involved in conceptualization, methodology, visualization, formal analysis, software, funding acquisition, investigation, writing—original draft, writing—review and editing; second author (Diana Salciarini) took part in conceptualization, funding acquisition and supervision, writing—review & editing; third author (Philip Vardon) involved in conceptualization, funding acquisition and supervision, writing—review and editing.

Funding Open access funding provided by Università degli Studi di Perugia within the CRUI-CARE Agreement.

Data Availability No datasets were generated or analyzed during the current study.

Declarations

Conflict of interest The authors declare no competing interests.

References

1. Abdelaziz S, Ozudogru TY (2016) Non-uniform thermal strains and stresses in energy piles. Environ Geotech 3(4):237–252. https://doi.org/10.1680/jenge.15.00032
2. Abdelaziz SL, Ozudogru TY (2016) Selection of the design temperature change for energy piles. Appl Therm Eng 107:1036–1045. https://doi.org/10.1016/j.applthermaleng.2016.07.067
3. Abdelaziz SL, Olgun CG, Martin II JR (2011) Design and operational considerations of geothermal energy piles. In Geofrontiers 2011: Advances in geotechnical engineering, pp. 450–459. https://doi.org/10.1061/41165(397)47
4. Agar JG, Morgenstern NR, Scott JD (1986) Thermal expansion and pore pressure generation in oil sands. Can Geotech J 23(3):327–333. https://doi.org/10.1139/t86-046
5. Batini N, Loria AFR, Conti P, Testi D, Grassi W, Laloui L (2015) Energy and geotechnical behaviour of energy piles for different design solutions. Appl Therm Eng 86:199–213. https://doi.org/10.1016/j.applthermaleng.2015.04.050
6. Bourne-Webb PJ, Amatya B, Soga K, Amis T, Davidson C, Payne P (2009) Energy pile test at Lambeth College, London: geotechnical and thermodynamic aspects of pile response to heat cycles. Géotechnique 59(3):237–248. https://doi.org/10.1680/geot.2009.59.3.237
7. Bourne-Webb PJ, Lupattelli A, Freitas TMB, Salciarini D (2022) The influence of initial shaft resistance mobilisation in the response of seasonally, thermally-activated pile foundations in granular media. Geomech Energy Environ 32:100299. https://doi.org/10.1016/j.gete.2021.100299
8. Brandl H (2006) Energy foundations and other thermo-active ground structures. Géotechnique 56(2):81–122. https://doi.org/10.1680/geot.2006.56.2.81
9. Campanella RG, Mitchell JK (1968) Influence of temperature variations on soil behavior. J Soil Mech Found Div 94(3):709–734. https://doi.org/10.1061/JSFEAQ.0001136
10. Cekerevac C, Laloui L (2004) Experimental study of thermal effects on the mechanical behaviour of a clay. Int J Numer Anal Meth Geomech 28(3):209–228. https://doi.org/10.1002/nag.332
11. De Santiago C, de Santayana FP, De Groot M, Urchueguía J, Badenes B, Magraner T, Arcos J, Martín F (2016) Thermo-mechanical behavior of a thermo-active precast pile. Bulg Chem Commun 48:41–54
12. Duffy K, Gavin K, Askarinejad A, Korff M, de Lange DA, Roubos AA (2022) Field testing of axially loaded piles in dense sand. In: Proceedings of the 20th International Conference on Soil Mechanics and Geotechnical Engineering, pp. 3253–3258
13. Faizal M, Bouazza A, Haberfield C, McCartney JS (2018) Axial and radial thermal responses of a field-scale energy pile under monotonic and cyclic temperature changes. J Geotech Geoenviron Eng 144(10):04018072. https://doi.org/10.1061/(ASCE)GT.1943-5606.0001952
14. Faizal M, Bouazza A, McCartney JS, Haberfield C (2019) Axial and radial thermal responses of energy pile under six storey residential building. Can Geotech J 56(7):1019–1033. https://doi.org/10.1139/cgj-2018-0246
15. Faizal M, Bouazza A, McCartney JS, Haberfield C (2019) Effects of cyclic temperature variations on thermal response of an energy pile under a residential building. J Geotech Geoenviron Eng 145(10):04019066. https://doi.org/10.1061/(ASCE)GT.1943-5606.0002147
16. Fang J, Kong G, Yang Q (2022) Group performance of energy piles under cyclic and variable thermal loading. J Geotech Geoenviron Eng 148(8):04022060. https://doi.org/10.1061/(ASCE)GT.1943-5606.0002840
17. Feng S, Fang J, Zhao Y, Zhang Z, Wang Y (2024) Thermomechanical analysis of energy piles using a load-transfer approach considering soil coupling effects. Comput Geotech 168:106147. https://doi.org/10.1016/j.compgeo.2024.106147
18. Gavin K, Kovacevic MS, Igoe D (2021) A review of CPT based axial pile design in the Netherlands. Undergr Space 6(1):85–99. https://doi.org/10.1016/j.undsp.2019.09.004
19. Gawecka KA, Taborda DM, Potts DM, Cui W, Zdravković L, Haji Kasri MS (2017) Numerical modelling of thermo-active piles in London Clay. Proc Inst Civ Eng Geotech Eng 170(3):201–219. https://doi.org/10.1680/jgeen.16.00096
20. Golchin A, Guo Y, Vardon PJ, Liu S, Zhang G, Hicks MA (2023) Shear creep behaviour of soil–structure interfaces under thermal

cyclic loading. Géotech Lett 13(1):22–28. https://doi.org/10.1680/jgele.22.00009
21. Guo Y, Golchin A, Hicks MA et al (2023) Experimental investigation of soil–structure interface behaviour under monotonic and cyclic thermal loading. Acta Geotech 18(7):3585–3608. https://doi.org/10.1007/s11440-022-01781-5
22. Jiang G, Lin C, Shao D, Huang M, Lu H, Chen G, Zong C (2021) Thermo-mechanical behavior of driven energy piles from full-scale load tests. Energy and Buildings 233:110668. https://doi.org/10.1016/j.enbuild.2020.110668
23. Jiang G, Shao D, Zong C, Chen G, Huang J, Lin C, Zhang Y (2023) Thermo-mechanical behavior of long-bored energy pile: a full-scale field investigation. KSCE J Civ Eng 27(1):145–155. https://doi.org/10.1007/s12205-022-0588-1
24. Kalantidou A, Tang AM, Pereira JM, Hassen G (2012) Preliminary study on the mechanical behaviour of heat exchanger pile in physical model. Géotechnique 62(11):1047–1051. https://doi.org/10.1680/geot.11.T.013
25. Kong G, Fang J, Huang X, Liu H, Abuel-Naga H (2021) Thermal induced horizontal earth pressure changes of pipe energy piles under multiple heating cycles. Geomech Energy Environ 26:100228. https://doi.org/10.1016/j.gete.2020.100228
26. Kong G, Li R, Deng H, Yang Q (2023) Behaviours of a belled energy pile under heating-cooling cycles. J Build Eng 72:106652. https://doi.org/10.1016/j.jobe.2023.106652
27. Laloui L, Nuth M, Vulliet L (2006) Experimental and numerical investigations of the behaviour of a heat exchanger pile. Int J Numer Anal Meth Geomech 30(8):763–781. https://doi.org/10.1016/B978-0-08-100191-2.00016-2
28. Li R, Kong G, Sun G, Zhou Y, Yang Q (2021) Thermomechanical characteristics of an energy pile-raft foundation under heating operations. Renew Energy 175:580–592. https://doi.org/10.1016/j.renene.2021.05.020
29. Liu HL, Wang CL, Kong GQ, Bouazza A (2019) Ultimate bearing capacity of energy piles in dry and saturated sand. Acta Geotech 14:869–879. https://doi.org/10.1007/s11440-018-0661-6
30. Loria AFR, Gunawan A, Shi C, Laloui L, Ng CW (2015) Numerical modelling of energy piles in saturated sand subjected to thermo-mechanical loads. Geomech Energy Environ 1:1–15. https://doi.org/10.1016/j.gete.2015.03.002
31. Luo J, Zhang Q, Zhao H, Gui S, Xiang W, Rohn J, Soga K (2019) Thermal and thermomechanical performance of energy piles with double U-loop and spiral loop heat exchangers. J Geotech Geoenviron Eng 145(12):04019109. https://doi.org/10.1061/(ASCE)GT.1943-5606.0002175
32. Lupattelli A, Bourne-Webb PJ, Bodas Freitas TM, Salciarini D (2023) A numerical study of the behavior of micropile foundations under cyclic thermal loading. Appl Sci 13(17):9791. https://doi.org/10.3390/app13179791
33. Lupattelli A, Salciarini D, Cecinato F, Veveakis M, Freitas TMB, Bourne-Webb PJ (2023) Temperature dependence of soil-structure interface behaviour in the context of thermally-activated piles: a review. Geomech Energy Environ. https://doi.org/10.1016/j.gete.2023.100521
34. Lv Z, Kong G, Liu H, Ng CW (2020) Effects of soil type on axial and radial thermal responses of field-scale energy piles. J Geotech Geoenviron Eng 146(10):06020018. https://doi.org/10.1061/(ASCE)GT.1943-5606.0002367
35. McCartney JS, Murphy KD (2012) Strain distributions in full-scale energy foundations (DFI young professor paper competition 2012). DFI J J Deep Found Inst 6(2):26–38. https://doi.org/10.1179/dfi.2012.008
36. McCartney JS, Murphy KD (2017) Investigation of potential dragdown/uplift effects on energy piles. Geomech Energy Environ 10:21–28. https://doi.org/10.1016/j.gete.2017.03.001
37. Morteza Zeinali S, Abdelaziz SL (2021) Thermal consolidation theory. J Geotech Geoenviron Eng 147(1):04020147. https://doi.org/10.1061/(ASCE)GT.1943-5606.0002423
38. Murphy KD, McCartney JS (2015) Seasonal response of energy foundations during building operation. Geotech Geol Eng 33:343–356. https://doi.org/10.1007/s10706-014-9802-3
39. Murphy KD, McCartney JS, Henry KS (2015) Evaluation of thermo-mechanical and thermal behavior of full-scale energy foundations. Acta Geotech 10:179–195. https://doi.org/10.1007/s11440-013-0298-4
40. Ng CWW, Ma QJ (2019) Energy pile group subjected to non-symmetrical cyclic thermal loading in centrifuge. Géotech Lett 9(3):173–177. https://doi.org/10.1680/jgele.18.00161
41. Ng CWW, Shi C, Gunawan A, Laloui L (2014) Centrifuge modelling of energy piles subjected to heating and cooling cycles in clay. Geotech Lett 4(4):310–316. https://doi.org/10.1680/geolett.14.00063
42. Ng CWW, Shi C, Gunawan A, Laloui L, Liu HL (2015) Centrifuge modelling of heating effects on energy pile performance in saturated sand. Can Geotech J 52(8):1045–1057. https://doi.org/10.1139/cgj-2014-0301
43. Ng CWW, Gunawan A, Shi C, Ma QJ, Liu HL (2016) Centrifuge modelling of displacement and replacement energy piles constructed in saturated sand: a comparative study. Géotech Lett 6(1):34–38. https://doi.org/10.1680/jgele.15.00119
44. Ng CW, Farivar A, Gomaa SMMH, Shakeel M, Jafarzadeh F (2021) Performance of elevated energy pile groups with different pile spacing in clay subjected to cyclic non-symmetrical thermal loading. Renew Energy 172:998–1012. https://doi.org/10.1016/j.renene.2021.03.108
45. Ng CW, Farivar A, Gomaa SM, Jafarzadeh F (2021) Centrifuge modeling of cyclic nonsymmetrical thermally loaded energy pile groups in clay. J Geotech Geoenviron Eng 147(12):04021146. https://doi.org/10.1061/(ASCE)GT.1943-5606.0002689
46. Nguyen VT, Tang AM, Pereira JM (2017) Long-term thermo-mechanical behavior of energy pile in dry sand. Acta Geotech 12:729–737. https://doi.org/10.1007/s11440-017-0539-z
47. NEN NPR 7201:2017 Geotechniek - Bepaling van het axiaal draagvermogen van funderingspalen door middel van proefbelasting (2017)
48. Pan Y, Coulibaly JB, Rotta Loria AF (2020) Thermally induced deformation of coarse-grained soils under nearly zero vertical stress. Géotech Lett 10(4):486–491. https://doi.org/10.1680/jgele.20.00013
49. Pan Y, Coulibaly JB, Rotta Loria AF (2022) An experimental investigation challenging the thermal collapse of sand. Géotechnique 74(3):296–306. https://doi.org/10.1680/jgeot.21.00309
50. Rafai M, Tang AM, Badinier T, Salciarini D, de Sauvage J (2023) Thermally induced shear displacement of sand-concrete interface under different stress levels. In: Symposium on Energy Geotechnics 2023. https://doi.org/10.59490/seg.2023.541
51. Rafai M, Lupattelli A, Salciarini D (2022) Finite element modelling of energy piles using different constitutive models for the soil. XI Incontro Annuale dei Giovani Ingegneri Geotecnici IAGIG 2022:83–86
52. Rafai M, Salciarini D, Vardon PJ (2024) Full-scale in-situ tests on a displacement cast in situ energy pile: effects of cyclic thermal loads under different mechanical load levels on pile stress and strain. Geomech Energy Environ. https://doi.org/10.1016/j.gete.2024.100606
53. Rafai M, Tang AM, Badinier T, De Sauvage J, Salciarini D (2024) Effect of thermal cycles on sand-concrete interface under constant shear stress. Can Geotech J. https://doi.org/10.1139/cgj-2023-0140

54. Rafai M, Salciarini D, Vardon PJ (2024) Thermo-mechanical response of a cast in situ displacement energy pile (No. EGU24-7965). Copernicus Meetings, https://doi.org/10.5194/egusphere-egu24-7965, 2024.
55. Ren LW, Ren JY, Han ZP, Xu J (2023) Field tests on the thermomechanical responses of PHC energy piles under cooling and loading conditions. Acta Geotech 18(1):429–444. https://doi.org/10.1007/s11440-022-01559-9
56. Sittidumrong J, Jotisankasa A, Chantawarangul K (2019) Effect of thermal cycles on volumetric behaviour of Bangkok sand. Geomech Energy Environ 20:100127. https://doi.org/10.1016/j.gete.2019.100127
57. Stewart MA, McCartney JS (2014) Centrifuge modeling of soil-structure interaction in energy foundations. J Geotech Geoenviron Eng 140(4):04013044. https://doi.org/10.1061/(ASCE)GT.1943-5606.0001061
58. Sutman M, Brettmann T, Olgun CG (2019) Full-scale in-situ tests on energy piles: head and base-restraining effects on the structural behaviour of three energy piles. Geomech Energy Environ 18:56–68. https://doi.org/10.1016/j.gete.2018.08.002
59. Wang B, Bouazza A, Singh RM, Haberfield C, Barry-Macaulay D, Baycan S (2015) Post-temperature effects on shaft capacity of a full-scale geothermal energy pile. J Geotech Geoenviron Eng 141(4):04014125. https://doi.org/10.1061/(ASCE)GT.1943-5606.0001266
60. Wang Y, Zhang F, Liu F, Wang X (2024) Full-scale in situ experimental study on the bearing capacity of energy piles under varying temperature and multiple mechanical load levels. Acta Geotech 19(1):401–415. https://doi.org/10.1007/s11440-023-01904-6
61. Yavari N, Tang AM, Pereira JM, Hassen G (2014) Experimental study on the mechanical behaviour of a heat exchanger pile using physical modelling. Acta Geotech 9:385–398. https://doi.org/10.1007/s11440-014-0310-7
62. Yavari N, Tang AM, Pereira JM, Hassen G (2016) Mechanical behaviour of a small-scale energy pile in saturated clay. Géotechnique 66(11):878–887. https://doi.org/10.1680/jgeot.15.T.026
63. Yazdani S, Helwany S, Olgun G (2019) Investigation of thermal loading effects on shaft resistance of energy pile using laboratory-scale model. J Geotech Geoenviron Eng 145(9):04019043. https://doi.org/10.1061/(ASCE)GT.1943-5606.0002088
64. Zhao R, Leung AK, Knappett JA (2022) Thermally induced ratcheting of a thermo-active reinforced concrete pile in sand under sustained lateral load. Géotechnique 73(9):826–839. https://doi.org/10.1680/jgeot.21.00299